Published in final edited form as:
Clin Cancer Res. 2014 May 15; 20(10): 2740–2750. doi:10.1158/1078-0432.CCR-13-2507.

Biological effects of platelet-derived growth factor receptor α blockade in uterine cancer

Ju-Won Roh[1,2,10], **Jie Huang**[1,10], **Wei Hu**[1,10], **XiaoYun Yang**[1], **Nicholas B. Jennings**[1], **Vasudha Sehgal**[3], **Bo Hwa Sohn**[3], **Hee Dong Han**[1], **Sun Joo Lee**[1,4], **Duangmani Thanapprapasr**[1,5], **Justin Bottsford-Miller**[1], **Behrouz Zand**[1], **Heather J. Dalton**[1], **Rebecca A. Previs**[1], **Ashley N. Davis**[1], **Koji Matsuo**[1,6], **Ju-Seog Lee**[3], **Prahlad Ram**[3], **Robert L. Coleman**[1], and **Anil K. Sood**[1,7,8,9]

[1]Department of Gynecologic Oncology and Reproductive Medicine, The University of Texas MD Anderson Cancer Center, Houston, TX [2]Department of Obstetrics & Gynecology, Dongguk University, Seoul, Korea [3]Department of Systems Biology, Konkuk University, Seoul, Korea [4]Department of Obstetrics & Gynecology, Konkuk University, Seoul, Korea [5]Department of Obstetrics and Gynecology, Ramathibodi Hospital, Mahidol University, Bangkok, Thailand [6]University of Southern California, Los Angeles, CA [7]Department of Cancer Biology, The University of Texas MD Anderson Cancer Center, Houston, TX [8]Center for RNA Interference and Non-Coding RNA, the University of Texas MD Anderson Cancer Center, Houston, TX

Abstract

Purpose—Platelet-derived growth factor receptor alpha (PDGFRα) expression is frequently observed in many kinds of cancer and is a candidate for therapeutic targeting. This preclinical study evaluated the biological significance of PDGFRα and PDGFRα blockade (using a fully humanized monoclonal antibody, 3G3) in uterine cancer.

Experimental Design—Expression of PDGFRα was examined in uterine cancer clinical samples and cell lines, and biological effects of PDGFRα inhibition were evaluated using *in vitro* (cell viability, apoptosis, and invasion) and *in vivo* (orthotopic) models of uterine cancer.

Results—PDGFRα was highly expressed and activated in uterine cancer samples and cell lines. Treatment with 3G3 resulted in substantial inhibition of PDGFRα phosphorylation and of downstream signaling molecules AKT and MAPK. Cell viability and invasive potential of uterine cancer cells were also inhibited by 3G3 treatment. In orthotopic mouse models of uterine cancer, 3G3 monotherapy had significant antitumor effects in PDGFRα-positive models (Hec-1A, Ishikawa, Spec-2), but not in PDGFRα-negative model (OVCA432). Greater therapeutic effects were observed for 3G3 in combination with chemotherapy than for either drug alone in the PDGFRα-positive models. The anti-tumor effects of therapy were related to increased apoptosis and decreased proliferation and angiogenesis.

[9]Corresponding Author: Dr. Anil K. Sood, Professor, Departments of Gynecologic Oncology and Cancer Biology, The University of Texas MD Anderson Cancer Center, 1155 Herman Pressler Blvd., Unit 1362, Houston, TX 77030, Phone: 713-745-5266, Fax: 713-792-7586, asood@mdanderson.org.
[10]These authors contributed equally to this work

Disclosure of Potential Conflicts of Interest: None of the authors has any conflicts of interest to disclose.

Conclusions—These findings identify PDGFRα as an attractive target for therapeutic development in uterine cancer.

Keywords

PDGFRα; 3G3; uterine cancer

Introduction

Uterine cancer is the most common gynecologic malignancy and the fourth most common cancer in North American women (1). Although overall outcome for these women is quite good, patients with recurrent or advanced-stage disease have a much poorer prognosis, with a median survival of 12 months (2). The mainstay of treatment for women with advanced disease remains systemic therapy in the form of hormonal agents or cytotoxic chemotherapy. Although tumor response to therapy has been documented, the treatments associated with intolerable side effects and infrequent durable remission (3). Therefore, new and more effective targeted therapies are needed.

Platelet-derived growth factor receptor α (PDGFRα) is a type III receptor tyrosine kinase that can be activated by PDGF-AA, PDGF-AB, PDGF-BB, and PDGF-CC (4, 5). These growth factors are dimeric molecules composed of disulfide-linked polypeptide chains that bind to two receptors simultaneously and induce receptor dimerization, autophosphorylation, and intracellular signaling. Activated receptors induce a variety of cellular signals that act to prevent apoptosis, stimulate mitogenesis, and promote cellular chemotaxis (6, 7). These effects are mediated through several well-characterized downstream signaling cascades, including the Ras/mitogen-activated protein kinase (MAPK) pathway and the phosphatidylinositol 3-kinase (PI3-K)/AKT pathway (8, 9). PDGFRα is critical to early development as evidenced by mice homozygous for a null mutation die during embryogenesis (10). In the adult, PDGFs function in wound healing by activating mitogenesis, chemotaxis, and protein synthesis of PDGFR-positive fibroblast and smooth muscle cells (11). Although these mesenchymal cells are considered to be “classic” targets for PDGFs, tumor cells have also been shown to express PDGFRs, providing evidence for the involvement of this receptor in tumorigenesis (12).

Tumors reported to express PDGFRα include ovarian (13), prostate (14), breast (15), lung (16), and melanoma (17). Also, tumor PDGFRα expression has been associated with disease progression in renal cell cancer (18), diminished survival in ovarian cancer (13), lymph node metastasis in breast cancer (19), and bone metastases in prostate cancer (20). The extracellular region of the receptor consists of five immunoglobulin-like domains while the intracellular part is a tyrosine kinase domain. The ligand-binding sites of the receptors are located in the first three immunoglobulin-like extracellular domains (6,7,21,22). Recently, a fully humanized monoclonal antibody to PDGFRα, called 3G3 (ImClone System, New York, NY), was developed. The epitopes for 3G3 spatially overlap the PDGF-AA and PDGF-BB binding sites, and strong affinity for PDGFRα was confirmed. The 3G3 antibody has been shown to inhibit ligand-induced dimerization and autophosphorylation, and promote PDGFR internalization after prolonged treatment (21). Moreover, therapeutic

efficacy with 3G3 has been in several malignancies including preclinical models of leiomyosarcoma and glioblastoma (22). However, in uterine cancer, the role of PDGFRα and the effect of its blockade have not yet been determined. The purpose of our study was to determine the biological and therapeutic effects of PDGFRα blockade in uterine cancer models.

Materials and Methods

Cell lines and cultures

Uterine cancer cell lines (HEC-265, SPEC-2,HEC1-A, Ishikawa, RL95-2, AN3CA, SKUT-2, and KLE) and ovarian cancer cell lines (SKOV3, OVCA432, OVCAR5, A2780, and HeyA8) were obtained from the MD Anderson Characterized Cell Line Core Facility (Houston, Texas), which supplies authenticated cell lines. Cells were maintained in specific culture medium. The cell lines were routinely tested to confirm the absence of mycoplasma, and all experiments were performed with cell lines at 60%–80% confluence. Before *in vivo* injection, cells were trypsinized, centrifuged at 1,100 rpm for 5 minutes at 4°C, washed twice with DPBS, and resuspended in HBSS for intrauterine injections. The cell lines were routinely tested to confirm the absence of mycoplasma, and all experiments were performed with cell lines at 60%–80% confluence.

Reagents

3G3 (neutralizing fully human immunoglobulin G monoclonal antibody to PDGFRα) was provided by ImClone Systems. Additional details regarding the development of this antibody have been described previously (21). Paclitaxel, docetaxel and cisplatin (cis-diamminedichloroplatinum, CDDP) were purchased from the MD Anderson Cancer Center pharmacy.

Western blot

Preparation of cell and tumor tissue lysates has been described previously (24). Protein concentrations were determined using a BCA Protein Assay Reagent Kit (Pierce Biotech, Rockford, IL), and aliquots of 30 μg protein were subjected to gel electrophoresis on 8 or 10% SDS-PAGE gels. Transfer to membranes and immunoblotting were performed as described previously (24). The following antibodies were used for Western blot analyses: PDGFRα (Cell Signaling, Danvers, MA, #3174), phospho-PDGFRα (pY^{762}) (Invitrogen, Camarillo, CA, #44–1010), MAPK and phospho-MAPK (pT^{202}/pY^{204}) (Cell Signaling, #9102, #9101), AKT and pAKT (pS^{473}) (Cell Signaling, #9272, #9746).

Receptor and downstream signaling molecule phosphorylation assays were done as described previously (21). Briefly, cells were seeded in 6-well tissue culture plates (1×10^6 cells per well) and allowed to grow overnight. The cells were then rendered quiescent by serum deprivation, treated with monoclonal antibodies for 2 hours at 37°C, and then stimulated with human PDGF-AA (R&D Systems, Minneapolis, MN) for 10 minutes at 37°C. Afterward, cell lysates were analyzed by SDS-PAGE and Western blotting with the antibodies mentioned above.

Cell viability assay

Cytotoxic effects of 3G3 compared to human immunoglobulin G (HmIgG) and to no treatment, with or without chemotherapy, were determined by the MTT uptake assay as described previously (25). Cells were plated on 96-well plates (7,000/well for Ishikawa, Hec-1A, and KLE, 10,000/well for Spec-2) in triplicate and incubated overnight at 37°C and 5% CO_2. After incubation, cells were washed, serum-free medium was added, and cells were treated with PBS (control), HmIgG, and 3G3. After 6 hours, regular media or media-containing chemotherapeutic agents (paclitaxel, docetaxel, and cisplatin) added. After 72 hours (Ishikawa, Hec-1A, or Spec-2) or 96 hours (KLE), cell viability was determined.

Apoptosis assay

The relative percentage of apoptotic cells was assessed by Phycoerythrin (PE) Annexin V and 7-amino-actinomycin (7-AAD) staining (BD Biosciences, San Diego, CA), as previously described (25). Briefly, uterine cancer cells (1×10^5 cells/mL) were pelleted and washed twice in PBS and resuspended in a binding buffer containing PE Annexin V and 7-AAD (5 μL per 10^5 cells). Samples were incubated in the dark for 15 minutes at room temperature before being analyzed by flow cytometry.

Cell invasion assay

Cell invasion assays have been previously described (15). Briefly, cells were treated with control, HmIgG, or 3G3 for 6 hours. Cells were then reconstituted in serum-free medium (1×10^6 cells/mL), and 100 μL added to inserts coated with a defined matrix consisting of human laminin, type IV collagen, and gelatin. Inserts were then transferred to wells filled with serum-containing media. Cells were then allowed to invade for 24 hours at 37°C. Cells that had migrated into the bottom wells were collected, fixed, stained, and counted by light microscopy. Cells were counted in 10 random fields (×200 final magnification) and the average number of cells determined.

Animal care and orthotopic implantation of tumor cells

Female athymic nude mice (NCr-nu) were purchased from the National Cancer Institute–Frederick Cancer Research and Development Center, and housed in specific pathogen-free conditions. They were cared for in accordance with guidelines set forth by the Association for Assessment and Accreditation of Laboratory Animal Care International and the U.S. PHS Policy on Humane Care and Use of Laboratory Animals, and all studies were approved and supervised by the MD Anderson Cancer Center Institutional Animal Care and Use Committee.

To produce tumors, Hec-1A and Ishikawa cells (both 4.0×10^6 cells per 50 μL HBSS) or Spec-2 cells (2.0×10^6 cells per 50 μL HBSS) (25) were injected into the mice. Before injection, mice were anesthetized with isoflurane inhalation (Baxter, Deerfield, IL), and a 0.5-cm incision was made in the right lower flank to optimize exposure to the right uterine horn. The distal portion of the horn was then identified and pulled to the incision for exposure. A single-cell suspension of 50 μL was then injected into the lumen of the uterine horn. The injection site was closely monitored during and following injection to ensure that no spillage occurred into the peritoneal cavity (23). The incision was then closed with

staples. Mice were monitored daily for adverse effects of therapy, and all were euthanized when any of the mice seemed moribund.

Therapy for established uterine tumors in nude mice

To assess tumor growth, treatment began two weeks after injection of tumor cells. Mice were randomly divided into 4 groups (n = 10 mice per group); (a) control PBS, (b) 3G3, (c) paclitaxel (Ishikawa, Hec-1A and OVCA432) or docetaxel (Spec-2), and (d) 3G3 combined with chemotherapy (paclitaxel or docetaxel).

Antibody 3G3 was dosed using 60 mg/kg intraperitoneal injection twice weekly with an initial loading dose of 214 mg/kg (21). Chemotherapy was injected into the peritoneal cavity once a week at a dose of 100 μg/mouse (paclitaxel) or 30 μg/mouse (docetaxel). Mice were euthanized after they became moribund (typically six to seven weeks, depending on tumor cell type). Tumor weight, number of tumor nodules, and distribution of tumors were recorded. Tumor tissue used in this study was obtained at the time of necropsy, and immersed in optimum cutting temperature medium for frozen slide preparations. Tumor specimens were also fixed in formalin for paraffin slide preparation.

Immunohistochemical staining

Expression of PDGFRα (Santa Cruz Biotechnology, CA, #sc-338), and pPDGFRα (pY720) (#sc-12910) was examined in clinical samples (10 normal endometrium, 10 endometrial polyp, and 20 endometrial cancers). For immunohistochemistry, staining was graded from 0 (no staining) to 3 (strong staining), based on the intensity and number of positive cells, by a single pathologist. Immunohistochemical analysis for CD31 and Ki67 was performed as previously described (26). To quantify microvessel density (MVD), the number of blood vessels staining positive for CD31 was recorded in five random fields at ×200 magnification for each sample. For Ki67, the number of positive cells and the total number of cells were counted in five random fields at ×200 magnification for each sample. Terminal deoxynucleotidyl transferase-mediated deoxyuridine triphosphate nick-end labeling (TUNEL) staining was performed on frozen tissue using a Promega Kit (Promega, Madison, WI), and cells were counted in five random fields at ×200 magnification (26).

Microarray Analysis of PDGFR downstream Genes

We analyzed the effect of 3G3 on differentially downregulated genes in the HEC1A and RL95-2 cells using the Illumina cDNA microarray platform. Briefly, HEC1A and RL95-2 cells were treated with 3G3 or PDGF-AA or the combination for 24 hours. For microarray hybridization, total RNA was extracted from treated and untreated cells using a mirVana RNA isolation labeling kit (Ambion, Austin, Texas). We used 750 ng of total RNA to label and hybridize the cells according to Illumina's protocols. After we scanned bead chips (Sentrix HumanHT-12 v3, Illumina) using an Illumina BeadArray reader, we normalized the microarray data using the quantile normalization method with the Linear Models for Microarray Data software program in the R language (Denton, Texas). The level of expression of each gene was transformed into a log2 base before additional analysis was performed. Genes that were differentially expressed in control and treated cells were identified using a random-variance t-test; gene-expression differences were considered

statistically significant if the p values were less than 0.001. A stringent significance threshold was used to limit the number of false-positive findings. In addition, the NetWalker software program was used for gene network analysis (35). In accordance with Minimum Information About a Microarray Experiment (MIAME) guidelines, we deposited the microarray data into the GEO repository with accession number GSE55483.

Statistical analyses

Continuous variables were assessed for normal distribution (Kolmogorov-Smirnov test) and expressed as appropriate (mean with SEM or median with range). A one-way ANOVA test with post hoc (Bonferroni adjustment) comparison or Kruskal-Wallis test with multiple comparisons (Wilcoxon rank sum test with Bonferroni correction) was performed to determine the statistical significance as appropriate. Categorical variables were evaluated with use of the Fisher's exact test. Three replicates were taken to monitor the performance of each experiment. We repeated experiments independently at least three times for statistical analysis. A *P* value of <0.05 was considered statistically significant. IBM SPSS Statistics 21.0 (IBM SPSS, Inc., Chicago, IL) was used for all statistical analyses.

Results

Basal expression of PDGFRα and anti-phosphorylation effect of its blockade

We first examined PDGFRα expression in uterine and ovarian cancer cell lines. All cells tested showed PDGFRα expression, except RL95-2 and OVCA432 cells (Fig. 1A). The effects on PDGF-induced intracellular signaling by anti-PDGFRα antibody 3G3 were determined using the PDGFRα positive cells (Hec-1A) and PDGFRα negative cells (RL95-2 and OVCA432). An early event in the signaling process is receptor autophosphorylation; therefore, 3G3 was tested for its ability to inhibit ligand-induced receptor tyrosine phosphorylation (Fig. 1B). PDGF-AA at 1 nmol/L concentration increased PDGFRα tyrosine phosphorylation. A higher concentration of ligand (PDGF-AA) (10 nmol/L) resulted in less receptor phosphorylation (data not shown), possibly because of ligand-induced degradation. The 3G3 antibody, at a concentration of 2 μg/mL or higher, inhibited PDGF-AA-induced receptor phosphorylation. As expected, PDGFRα blockade resulted in decreased phosphorylation of downstream proteins MAPK and AKT (Fig. 1B) in HEC1A cells, but no effects of 3G3 on AKT, p-AKT, MAPK and p-MAPK were noted in PDGFRα null cells (Fig. 1C). To determine PDGFRα expression in cancer and stromal populations, immunohistochemical staining of normal endometrium, endometrial polyps, and endometrial cancer samples was performed. There was higher expression of total and phospho-PDGFRα in cancer tissues compared to the benign controls (Supplementary Figure 1). Moreover, while there was some staining in the stroma, the predominant staining was present in the cancer cells (Supplementary Figure 1).

In vitro effect of PDGFRα blockade

Before testing the *in vivo* biological effect of PDGFRα blockade, we tested the *in vitro* effects on uterine cancer cell lines. To confirm the effect of 3G3, cell lines were tested at doses ranging from 0.1 to 200 μg/mL. Cell viability was inhibited by 3G3 alone in HEC1A, but not in RL95-2 cells (Fig. 2A). We also examined the effects of PDGFRα blockade using

the combination of 3G3 and chemotherapy (paclitaxel, docetaxel, and cisplatin; Fig. 2B). Treatment with 3G3 enhanced the cytotoxicity of chemotherapy in Ishikawa, Hec-1A, and Spec-2 cells, but not in KLE cells. In the Hec-1A and Spec-2 cell lines, combining all types of chemotherapy with 3G3 resulted in lower cell viabilities than were seen when the chemotherapy agents were combined with HmIgG or control. Statistical analysis showed that 3G3 enhanced the sensitivity to all chemotherapy drugs tested in the Ishikawa, Hec-1A, and Spec-2 cells, but still not in KLE cells (Fig.2C).

We next assessed whether PDGFRα blockade could promote tumor cell apoptosis. Although we did not find significant changes in apoptosis after co-treatment with 3G3 and PDGFAA in Hec1A and RL95-2 cells (Fig. 3A), pretreatment with 3G3 resulted in significantly increased tumor apoptosis in HEC1A cells, but not in RL95-2 cells (Fig.3A). Furthermore, combination of 3G3 with chemotherapy resulted in significantly increased tumor cell apoptosis in Ishikawa, Hec-1A, and Spec-2 cells, but not in KLE cells (Fig. 3B). These results paralleled the results of the cell viability assay. We also examined the effect of PDGFRα blockade on cancer cell invasion. Serum-deprivation decreased invasive ability, and PDGF-AA restored invasion in Ishikawa and HEC-1A cells. PDGFRα blockade with 3G3 resulted in significantly decreased cell invasion compared with controls in Ishikawa, Hec-1A, and Spec-2 cells (Fig. 4).

Therapeutic effect of PDGFRα blockade

Based on the *in vitro* data, we next assessed *in vivo* effects of PDGFRα blockade. Two weeks after orthotopic injection of tumor cells into the uterine horn, mice were randomly allocated to 1 of 4 treatment groups. Mice were euthanized when animals in any group became moribund. Both 3G3 alone and chemotherapy alone resulted in significant growth inhibition compared with PBS, as expected (89.8% and 86.6%, respectively, in Ishikawa cells; 50.9% and 71.7% in Hec-1A; 71.4% and 65.9% in Spec-2; Fig. 5A). The combination of 3G3 and chemotherapy resulted in the greatest tumor reduction compared with PBS (98.8% in Ishikawa, $P = 0.0004$; 84.5% in Hec-1A, $P < 0.0001$; 93.2% in Spec-2, $P = 0.011$). To identify the biological effects of PDGFRα blockade, we examined PDGFRα and phosphorylated PDGFRα, pAKT and pMAPK expression, tumor cell proliferation (Ki67), tumor-associated MVD (CD31 staining), and tumor cell apoptosis (TUNEL) (Fig. 5B and Supplementary Fig. S2). PDGFRα expression, especially the phosphorylated form, was significantly reduced in the 3G3 and combination groups. Moreover, there was reduced expression of pAKT and pMAPK in the 3G3 treatment groups. Tumor cell proliferation was significantly reduced in the 3G3 group, chemotherapy group, and the combination group compared with the PBS group (20.3%, 21.2%, and 39.3% reduction, respectively, in the Hec-1A model, $P < 0.0001$; Fig. 5B). The decrease in the combination group was greatest and statistically significant in comparison to the 3G3- and paclitaxel-only groups ($P = 0.001$ and 0.0004, respectively; Fig. 5B). MVD was also significantly reduced in the 3G3, paclitaxel, and combination groups (53.1%, 63.65%, and 77.9% reduction, respectively, $P < 0.01$; Fig. 5B), and the combination group showed significantly lower MVD compared with the 3G3- and paclitaxel-only groups ($P < 0.0001$ and 0.004, respectively; Fig. 5B). Tumor cell apoptosis in the 3G3, paclitaxel, and combination groups was significantly increased compared with the PBS group in Hec-1A cells ($P < 0.0001$; Fig. 5B). Combination 3G3 and

paclitaxel treatment resulted in the greatest increase in tumor cell apoptosis compared with the 3G3-only, paclitaxel-only, and PBS groups ($P < 0.0001$; Fig. 5B). Similar observations were found in the Ishikawa and Spec-2 models (Supplementary Fig. S2).

To determine whether PDGFRα expression was necessary for the 3G3 therapeutic response, we carried out an experiment with the OVCA432 model (this model was used since the RL95-2 cell line is not tumorigenic in mouse models). In the OVCA432 model, no significant anti-tumor effect of 3G3 was observed (Figure 5A).

Since the *in vivo* effects of 3G3 therapy were greater than the observed *in vitro* effects, we considered the possibility of indirect effects on the tumor microenvironment *via* reduced production of angiogenesis factors by cancer cells. To address this possibility, we performed microarray analysis of PDGFRα-positive and -negative cells following treatment with 3G3. Integrated pathway analysis showed that several proangiogenic genes (e.g., VEGFA, HADC7, ITG and VCAN) were downregulated in PDGFRα positive cells, but not in negative cells (Figure 6).

Discussion

The key findings from this study are that PDGFRα blockade effectively inhibits growth in PDGFRα-positive uterine cancer models. PDGFRα has been considered an important target in other cancers including ovarian (13), prostate (14), breast (27), and lung (16). PDGF/PDGFRα signaling plays a relevant role in cancer biology not only because of direct effects on tumor cells but also because of paracrine effects mediated by PDGFRα expression on stromal cells (28–30). Here, while there were modest effects with 3G3 *in vitro,* the effects were more substantial *in vivo.* The differences in the *in vitro* vs. *in vivo* effects are likely explained by modulation of proangiogenic genes in PDGFRα positive cells following 3G3 treatment. Collectively, these data support both direct and indirect effects of the 3G3 antibody in uterine cancer models.

Antibody-based approaches may have some advantages over small molecules, including greater target specificity, less off-target toxicity, and an additional capacity for immune-mediated cytotoxicity (31). The 3G3 antibody is a neutralizing monoclonal antibody to PDGFRα and does not cross-react with the β-form of the receptor. 3G3 blocks both PDGF-AA and PDGF-BB ligands from binding to PDGFRα and receptor autophosphorylation. In addition to these functions, 3G3 has been shown to inhibit phosphorylation of downstream signaling molecules AKT and MAPK (21). AKT and MAPK have also been shown to play a role in response to chemotherapy in uterine cancer (32). The enhanced efficacy of 3G3 in combination with chemotherapy is likely due to blockade of these pathways (33). 3G3 treatment effectively inhibited autophosphorylation of receptor and phosphorylation of downstream molecules MAPK and AKT in PDGFRα positive cells, but not in PDGFRα null cells, suggesting that PDGFRα expression on cancer cells was an important determinant of response to 3G3.(34)

To date, clinical results with 3G3 reveal a favorable safety and therapeutic profile in patients with advanced solid tumors and lymphomas (30). On the basis of these preclinical and early

clinical findings, several phase II clinical trials of 3G3 in advanced solid malignancies are either underway or in development. In the future, combination studies of PDGFR-targeting therapeutics with anti-angiogenic agents may take further advantage of the potential interplay among tumor, stromal, and angiogenic factors that appear to be a hallmark of PDGFR signaling.

In summary, we demonstrated that inhibition of PDGFRα with 3G3 is an effective approach for treatment of uterine cancer in orthotopic animal models. PDGFRα blockade decreased tumor angiogenesis, cell survival, and tumor growth, and these effects might be related to modulated AKT and MAPK activity. These data suggest that this monoclonal antibody to PDGFRα may be useful for the treatment of uterine tumors that express PDGFRα.

Supplementary Material

Refer to Web version on PubMed Central for supplementary material.

Acknowledgments

We thank Sunita Patterson of the MD Anderson Department of Scientific Publications for the helpful editing..

Grant Support

National Institutes of Health (CA109298, P50 CA098258, P50 CA083639, CA128797, RC2GM092599, U54 CA151668, institutional Core Grant CA016672), Ovarian Cancer Research Fund, Inc. (Program Project Development Grant), U.S. Department of Defense (OC073399, OC093146), Anne Asche Murray Distinguished Professorship, and Laura and John Arnold Foundation. JBM, BZ, and HJD are supported by an NCI-DHHS-NIH T32 Training Grant (T32 CA101642). JR is supported by Basic Science Research Program of Korea funded by the Ministry of Education (NRF-2012R1A1A3014174).

References

1. Siegel R, Naishadham D, Jemal A. Cancer statistics, 2013. CA: a cancer journal for clinicians. 2013; 63:11–30. [PubMed: 23335087]
2. Obel JC, Friberg G, Fleming GF. Chemotherapy in endometrial cancer. Clinical advances in hematology & oncology : H&O. 2006; 4:459–468.
3. Humber CE, Tierney JF, Symonds RP, Collingwood M, Kirwan J, Williams C, et al. Chemotherapy for advanced, recurrent or metastatic endometrial cancer: a systematic review of Cochrane collaboration. Annals of oncology : official journal of the European Society for Medical Oncology / ESMO. 2007; 18:409–420. [PubMed: 17150999]
4. Heldin CH, Westermark B. Mechanism of action and in vivo role of platelet-derived growth factor. Physiol Rev. 1999; 79:1283–1316. [PubMed: 10508235]
5. Li X, Ponten A, Aase K, Karlsson L, Abramsson A, Uutela M, et al. PDGF-C is a new protease-activated ligand for the PDGF alpha-receptor. Nat Cell Biol. 2000; 2:302–309. [PubMed: 10806482]
6. Koyama H, Nishizawa Y, Hosoi M, Fukumoto S, Kogawa K, Shioi A, et al. The fumagillin analogue TNP-470 inhibits DNA synthesis of vascular smooth muscle cells stimulated by platelet-derived growth factor and insulin-like growth factor-I. Possible involvement of cyclin-dependent kinase 2. Circulation research. 1996; 79:757–764. [PubMed: 8831499]
7. Ekman S, Thuresson ER, Heldin CH, Ronnstrand L. Increased mitogenicity of an alphabeta heterodimeric PDGF receptor complex correlates with lack of RasGAP binding. Oncogene. 1999; 18:2481–2488. [PubMed: 10229199]

8. Vanhaesebroeck B, Leevers SJ, Panayotou G, Waterfield MD. Phosphoinositide 3-kinases: a conserved family of signal transducers. Trends in biochemical sciences. 1997; 22:267–272. [PubMed: 9255069]
9. Plattner R, Kadlec L, DeMali KA, Kazlauskas A, Pendergast AM. c-Abl is activated by growth factors and Src family kinases and has a role in the cellular response to PDGF. Genes & development. 1999; 13:2400–2411. [PubMed: 10500097]
10. Soriano P. The PDGF alpha receptor is required for neural crest cell development and for normal patterning of the somites. Development. 1997; 124:2691–2700. [PubMed: 9226440]
11. Ostman A, Heldin CH. Involvement of platelet-derived growth factor in disease: development of specific antagonists. Adv Cancer Res. 2001; 80:1–38. [PubMed: 11034538]
12. Fleming TP, Saxena A, Clark WC, Robertson JT, Oldfield EH, Aaronson SA, et al. Amplification and/or overexpression of platelet-derived growth factor receptors and epidermal growth factor receptor in human glial tumors. Cancer Res. 1992; 52:4550–4553. [PubMed: 1322795]
13. Henriksen R, Funa K, Wilander E, Backstrom T, Ridderheim M, Oberg K. Expression and prognostic significance of platelet-derived growth factor and its receptors in epithelial ovarian neoplasms. Cancer Res. 1993; 53:4550–4554. [PubMed: 8402626]
14. Fudge K, Wang CY, Stearns ME. Immunohistochemistry analysis of platelet-derived growth factor A and B chains and platelet-derived growth factor alpha and beta receptor expression in benign prostatic hyperplasias and Gleason-graded human prostate adenocarcinomas. Mod Pathol. 1994; 7:549–554. [PubMed: 7524068]
15. de Jong JS, van Diest PJ, van der Valk P, Baak JP. Expression of growth factors, growth-inhibiting factors, and their receptors in invasive breast cancer. II: Correlations with proliferation and angiogenesis. J Pathol. 1998; 184:53–57. [PubMed: 9582527]
16. Zhang P, Gao WY, Turner S, Ducatman BS. Gleevec (STI-571) inhibits lung cancer cell growth (A549) and potentiates the cisplatin effect in vitro. Mol Cancer. 2003; 2:1. [PubMed: 12537587]
17. Barnhill RL, Xiao M, Graves D, Antoniades HN. Expression of platelet-derived growth factor (PDGF)-A, PDGF-B and the PDGF-alpha receptor, but not the PDGF-beta receptor, in human malignant melanoma in vivo. Br J Dermatol. 1996; 135:898–904. [PubMed: 8977709]
18. Sulzbacher I, Birner P, Traxler M, Marberger M, Haitel A. Expression of platelet-derived growth factor-alpha alpha receptor is associated with tumor progression in clear cell renal cell carcinoma. American journal of clinical pathology. 2003; 120:107–112. [PubMed: 12866380]
19. Carvalho I, Milanezi F, Martins A, Reis RM, Schmitt F. Overexpression of platelet-derived growth factor receptor alpha in breast cancer is associated with tumour progression. Breast cancer research : BCR. 2005; 7:R788–R795. [PubMed: 16168125]
20. Chott A, Sun Z, Morganstern D, Pan J, Li T, Susani M, et al. Tyrosine kinases expressed in vivo by human prostate cancer bone marrow metastases and loss of the type 1 insulin-like growth factor receptor. The American journal of pathology. 1999; 155:1271–1279. [PubMed: 10514409]
21. Loizos N, Xu Y, Huber J, Liu M, Lu D, Finnerty B, et al. Targeting the platelet-derived growth factor receptor alpha with a neutralizing human monoclonal antibody inhibits the growth of tumor xenografts: implications as a potential therapeutic target. Mol Cancer Ther. 2005; 4:369–379. [PubMed: 15767546]
22. Shah GD, Loizos N, Youssoufian H, Schwartz JD, Rowinsky EK. Rationale for the development of IMC-3G3, a fully human immunoglobulin G subclass 1 monoclonal antibody targeting the platelet-derived growth factor receptor alpha. Cancer. 2010; 116:1018–1026. [PubMed: 20127943]
23. Kamat AA, Merritt WM, Coffey D, Lin YG, Patel PR, Broaddus R, et al. Clinical and biological significance of vascular endothelial growth factor in endometrial cancer. Clinical cancer research : an official journal of the American Association for Cancer Research. 2007; 13:7487–7495. [PubMed: 18094433]
24. Mangala LS, Zuzel V, Schmandt R, Leshane ES, Halder JB, Armaiz-Pena GN, et al. Therapeutic Targeting of ATP7B in Ovarian Carcinoma. Clinical cancer research : an official journal of the American Association for Cancer Research. 2009; 15:3770–3780. [PubMed: 19470734]
25. Lee JW, Han HD, Shahzad MM, Kim SW, Mangala LS, Nick AM, et al. EphA2 immunoconjugate as molecularly targeted chemotherapy for ovarian carcinoma. Journal of the National Cancer Institute. 2009; 101:1193–1205. [PubMed: 19641174]

26. Spannuth WA, Nick AM, Jennings NB, Armaiz-Pena GN, Mangala LS, Danes CG, et al. Functional significance of VEGFR-2 on ovarian cancer cells. International journal of cancer Journal international du cancer. 2009; 124:1045–1053. [PubMed: 19058181]
27. de Jong JS, van Diest PJ, van der Valk P, Baak JP. Expression of growth factors, growth inhibiting factors, and their receptors in invasive breast cancer. I: An inventory in search of autocrine and paracrine loops. J Pathol. 1998; 184:44–52. [PubMed: 9582526]
28. Alvarez RH, Kantarjian HM, Cortes JE. Biology of platelet-derived growth factor and its involvement in disease. Mayo Clinic proceedings. 2006; 81:1241–1257. [PubMed: 16970222]
29. Matei D, Satpathy M, Cao L, Lai YC, Nakshatri H, Donner DB. The platelet-derived growth factor receptor alpha is destabilized by geldanamycins in cancer cells. The Journal of biological chemistry. 2007; 282:445–453. [PubMed: 17079230]
30. Stock P, Monga D, Tan X, Micsenyi A, Loizos N, Monga SP. Platelet-derived growth factor receptor-alpha: a novel therapeutic target in human hepatocellular cancer. Mol Cancer Ther. 2007; 6:1932–1941. [PubMed: 17604334]
31. Imai K, Takaoka A. Comparing antibody and small-molecule therapies for cancer. Nature reviews Cancer. 2006; 6:714–727.
32. Li Z, Min W, Gou J. Knockdown of cyclophilin A reverses paclitaxel resistance in human endometrial cancer cells via suppression of MAPK kinase pathways. Cancer chemotherapy and pharmacology. 2013; 72:1001–1011. [PubMed: 24036847]
33. Matsuo K, Nishimura M, Komurov K, Shahzad MM, Ali-Fehmi R, Roh JW, et al. Platelet-derived growth factor receptor alpha (PDGFRalpha) targeting and relevant biomarkers in ovarian carcinoma. Gynecologic oncology. 2013
34. Killion JJ, Radinsky R, Fidler IJ. Orthotopic models are necessary to predict therapy of transplantable tumors in mice. Cancer metastasis reviews. 1998; 17:279–284. [PubMed: 10352881]
35. Komurov K, Dursun S, Erdin S, Ram PT. Software NetWalker: a contextual network analysis tool for functional genomics. BMC Genomics. 2012; 13:282–291. [PubMed: 22732065]

Translational Relevance

Platelet-derived growth factor receptor alpha (PDGFRα) expression is frequently observed in many kinds of cancer and is a candidate for therapeutic targeting. Here, we evaluated the biological significance of PDGFRα and PDGFRα blockade (using a fully humanized monoclonal antibody, 3G3) in uterine cancer. PDGFRα was expressed in uterine cancer cells, and its blockade with 3G3 resulted in inhibition of PDGFRα phosphorylation and of downstream signaling molecules, AKT and MAPK. Cell viability and invasive potential of uterine cancer cells were also inhibited by treatment of 3G3. Moreover, greater therapeutic effects were observed for 3G3 in combination with chemotherapy than for either drug alone in orthotopic mouse models of uterine cancer. These findings identify PDGFRα as an attractive therapeutic target for uterine cancer.

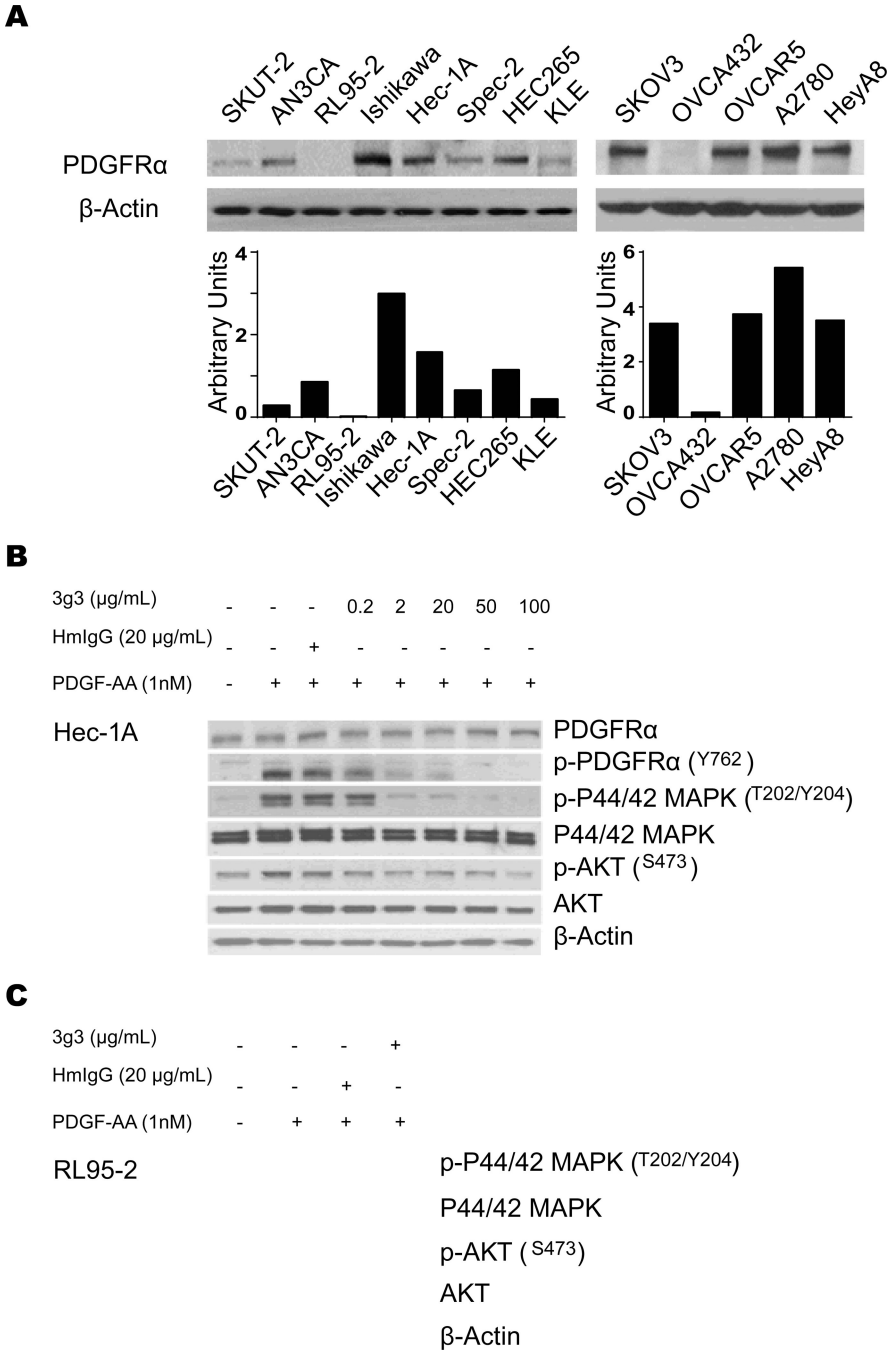

Figure 1. Expression of PDGFRa and anti-phosphorylation effect of its blockade in cancer cells

A, Western blot analysis of PDGFRa expression in uterine and ovarian cancer cell lines. B, In vitro effect of 3G3 on PDGFRa, pPDGFRa, and its downstream targets. Cells (Hec-1A) were treated with 3G3 or nonspecific human immunoglobulin G (HmIgG) for 24 hours and then stimulated with 1 nM PDGF-AA for 10 minutes. Cell lysates were analyzed by Western blot analysis with antibodies against PDGFRa, pPDGFRa, p 44/42 MAPK, MAPK, pAKT, and AKT. C, Western blot analysis of expression of PDGFRa downstream targets in RL95-2

cells. RL95-2 cells were treated with 3G3 or PDGF-AA as mentioned above. Loading of an equal amount of sample per gel lane was confirmed by b-actin expression.

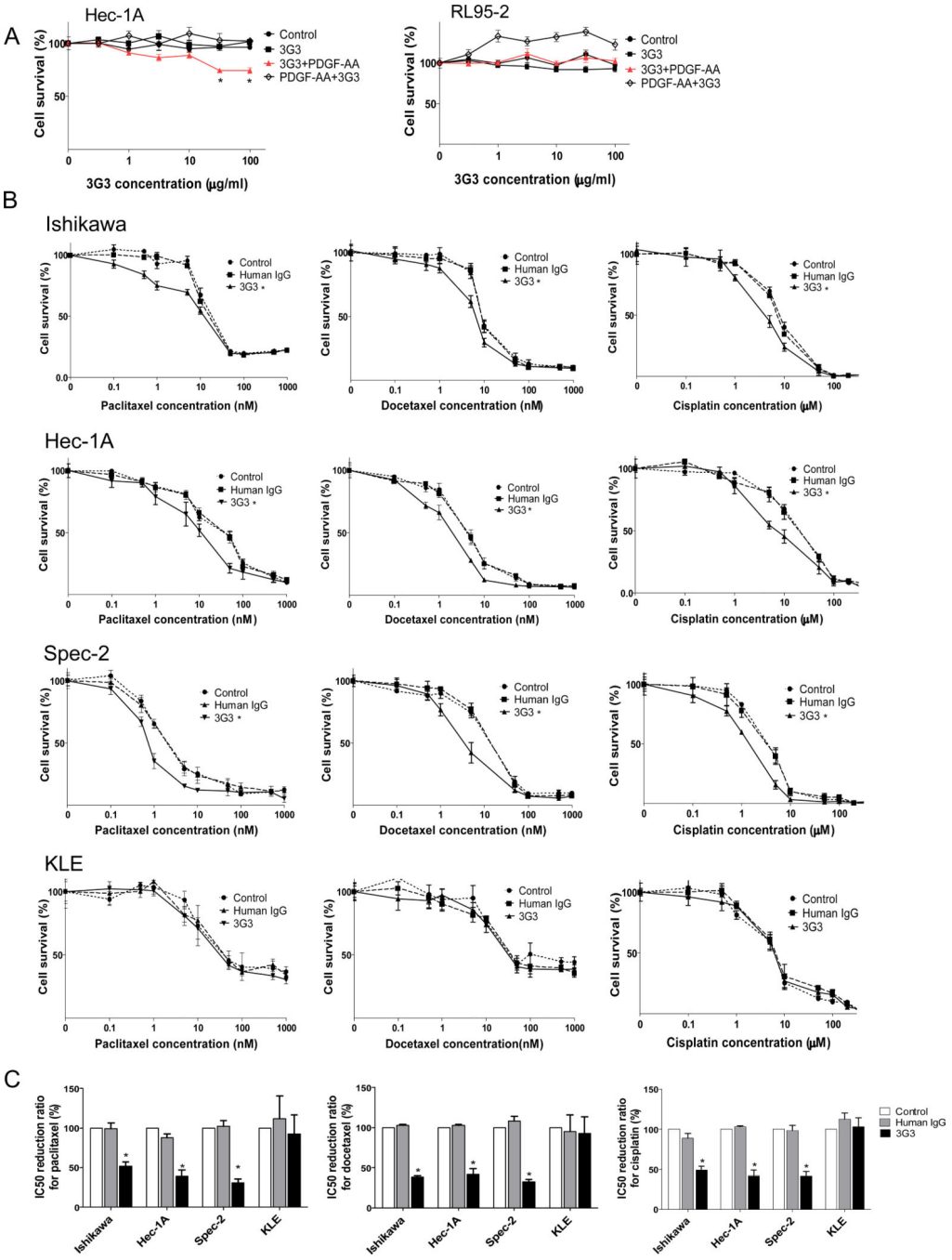

Figure 2. In vitro effects of 3G3 or the combination of 3G3 and chemotherapy on cell viability

A, MTT cell viability assay of HEC-1A and RL95-2 cells. Viability was assessed with the MTT assay at 72 hours after PDGF-AA stimulation or 3G3+PDGF-AA stimulation. '3G3+PDGF-AA' means pretreatment with 3G3 before PDGF-AA stimulation (red line), and 'PDGF-AA+3G3' means co-treatment with PDGF-AA and 3G3 at the same time. B, MTT cell viability assay of Ishikawa, Hec-1A, Spec-2, and KLE cells after 3G3 treatment combined with chemotherapy. C, IC50 reduction ratio of chemotherapy combined with 3G3

treatment. All experiments were statistically analyzed based on three repeated experiments. Error bars, SEM, and *, $P < 0.05$.

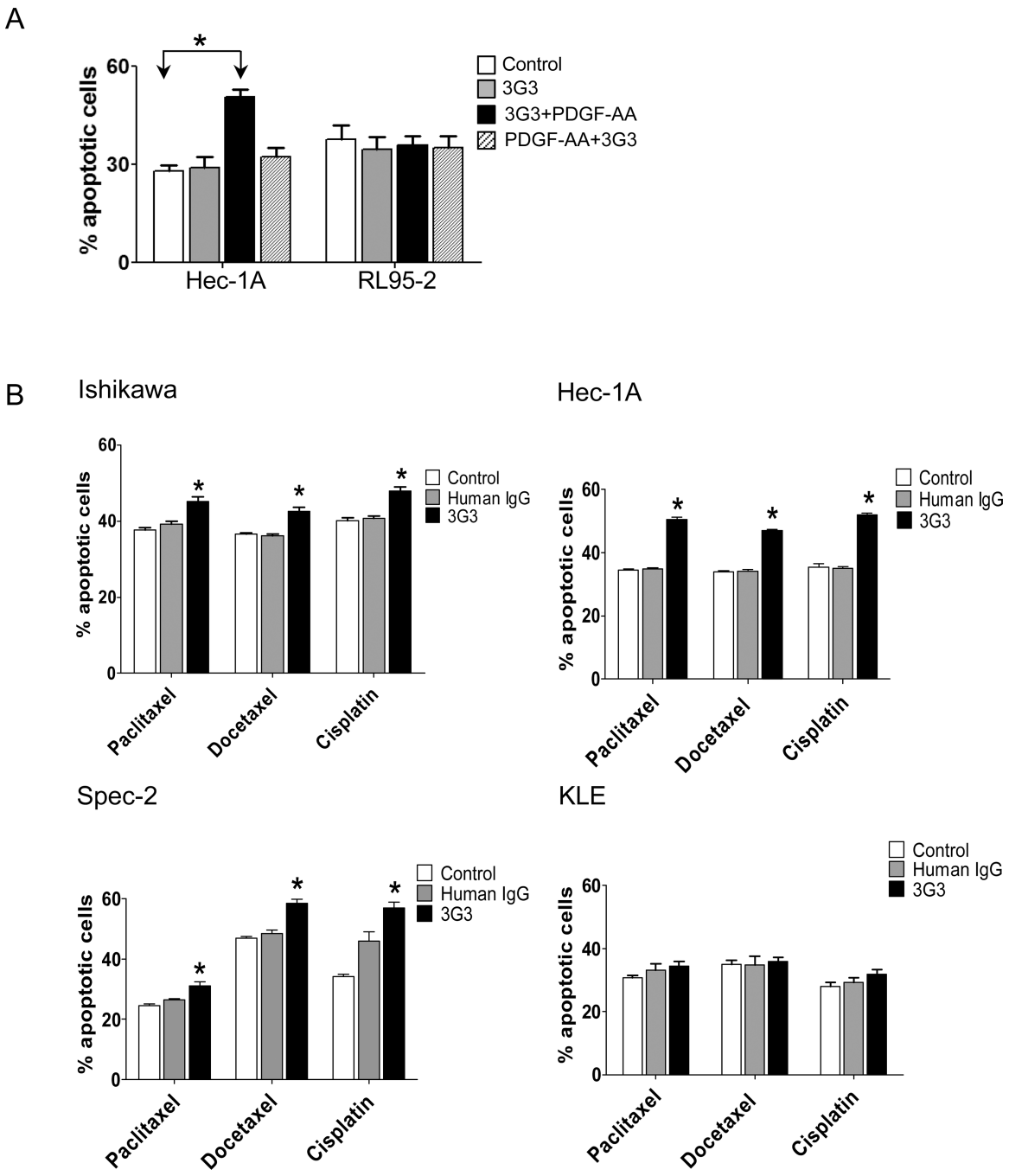

Figure 3. Effect of 3G3 or the combination of 3G3 and chemotherapy on apoptosis

A, Apoptosis of Hec-1A and RL95-2 cells was measured after treatment with 3G3 and PDGF-AA. '3G3+PDGF-AA' means pretreatment with 3G3 before PDGF-AA stimulation, and 'PDGF-AA+3G3' means co-treatment with PDGF-AA and 3G3 at the same time. B, Apoptosis of Ishikawa, Hec-1A, Spec-2, and KLE cells after pretreatment with 3G3 followed by cytotoxic chemotherapy. Apoptosis was measured by determining the percentage of PE Annexin V/7-AAD-positive cells at 72 hours after treatment. Statistical analysis was performed based on five repeated experiments. Error bars, SEM. *, $P < 0.05$.

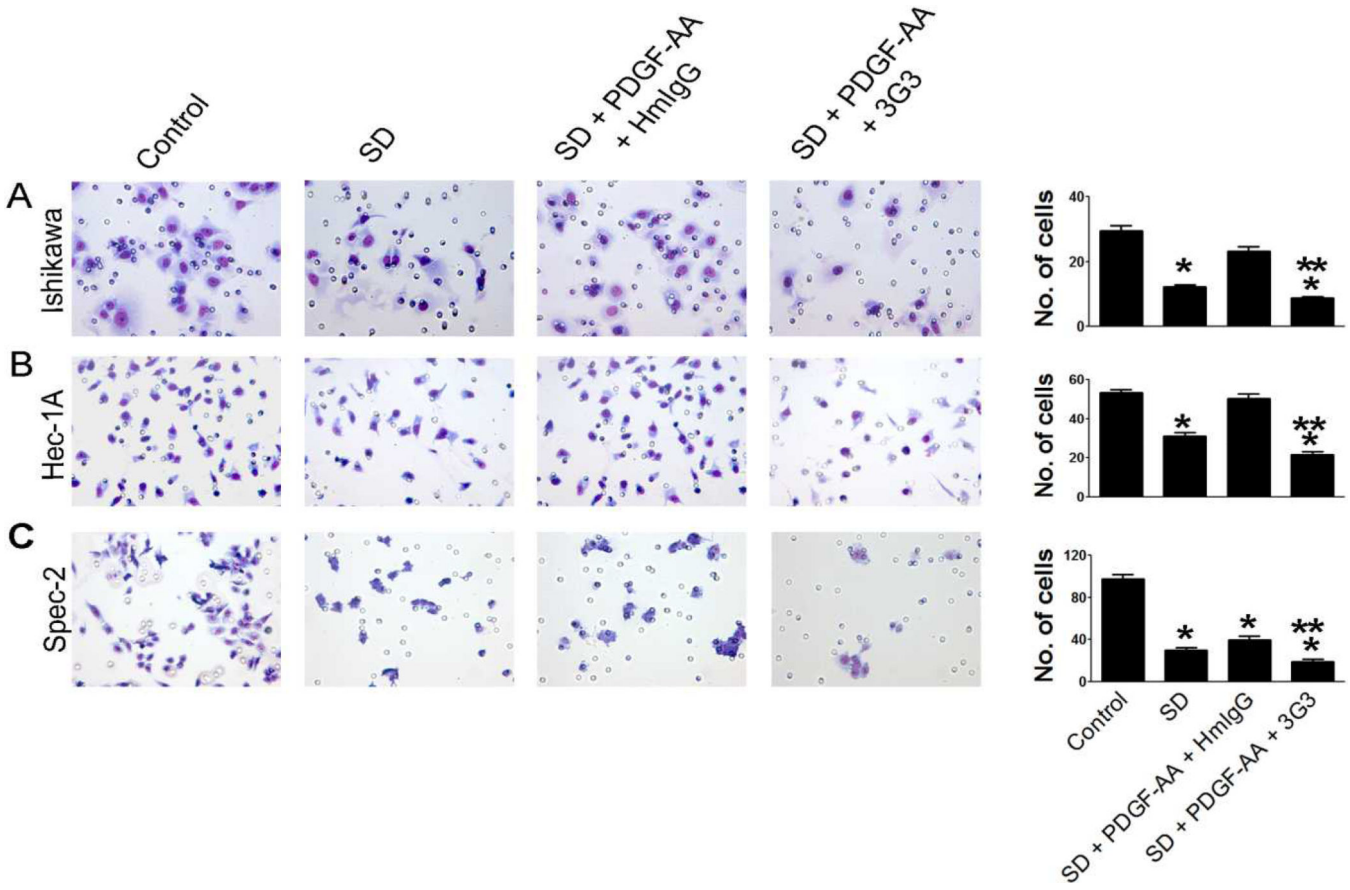

Figure 4. Effect of PDGFRα blockade on cell invasion in Ishikawa (A), Hec-1A (B), and Spec-2 cells (C)

PDGF-AA was used to activate PDGFRα expression. Statistical analysis was based on three repeated experiments. Error bars, SEM. *, $P < 0.05$ compared to control. **, $P < 0.05$ compared to serum deprivation (SD) condition.

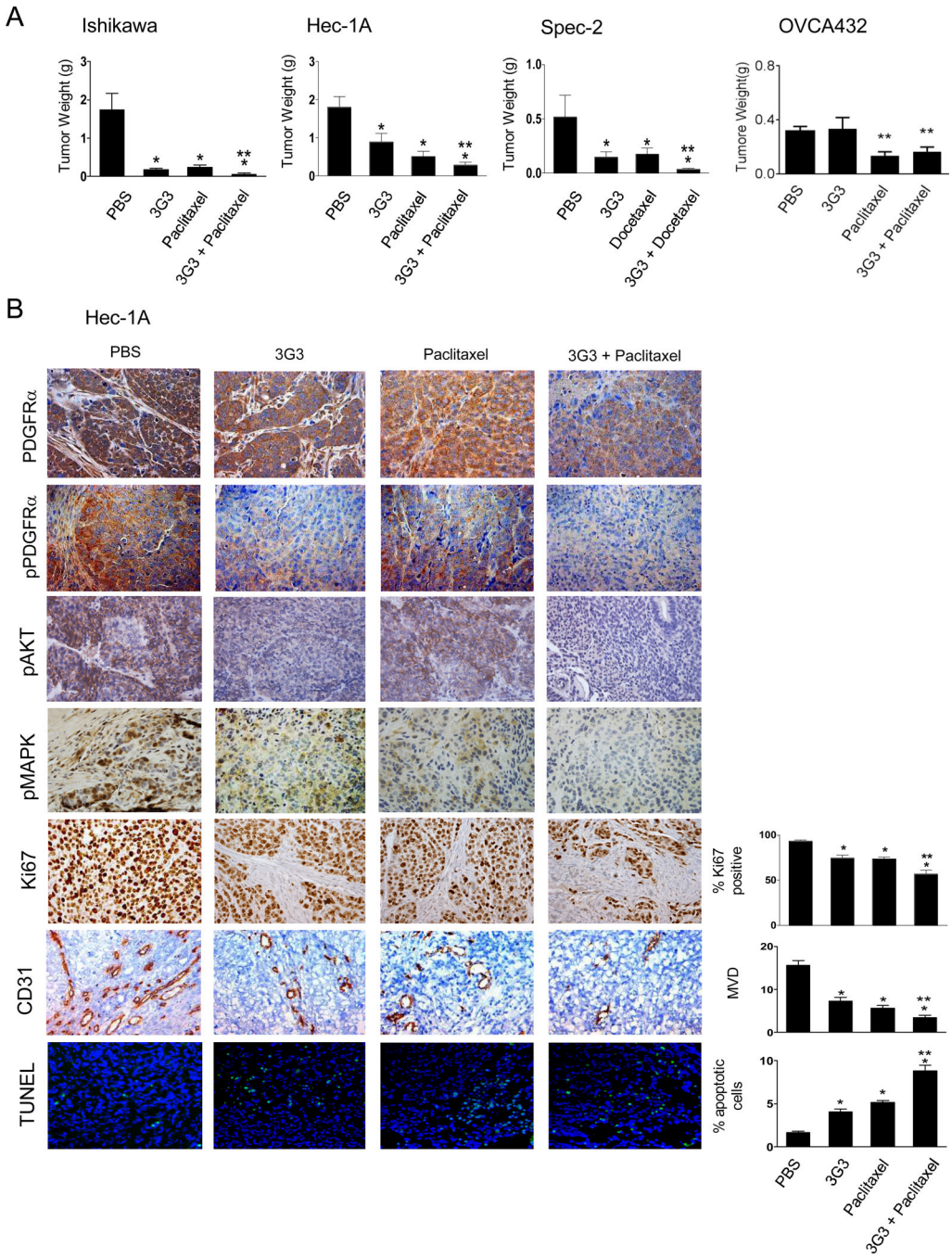

Figure 5. *In vivo* therapeutic and biological effects of PDGFRα blockade on uterine cancer

A, *In vivo* therapeutic effect of PDGFRα blockade on uterine cancer. Mice inoculated with Ishikawa, Hec-1A, Spec-2, or OVCA432 cells received PBS (control), 3G3 (a monoclonal antibody to human PDGFRα), chemotherapy (100 μg/mouse of paclitaxel or 30 μg/mouse of docetaxel), or a combination of 3G3 and chemotherapy 2 weeks following cell injection. Animals from all groups were euthanized when control animals became moribund (4–5 weeks after initiating therapy, depending on the cell line used). All tumors were harvested; mean tumor weight, number of nodules, and their distribution were recorded. Columns mean

tumor weights for each group; Error bars, SEM. * $P < 0.05$. B, In vivo biological effects of PDGFRα blockade on expression of PDGFRα, pPDGFRα, pAKT, and pMAPK; tumor cell proliferation (Ki67); angiogenesis (CD31); and apoptosis (TUNEL). Immunohistochemical stains were performed on Hec-1A cell-bearing mice. Error bars, SEM. *, $P < 0.05$ compared to control. **, $P < 0.05$ compared to chemotherapy-alone group.

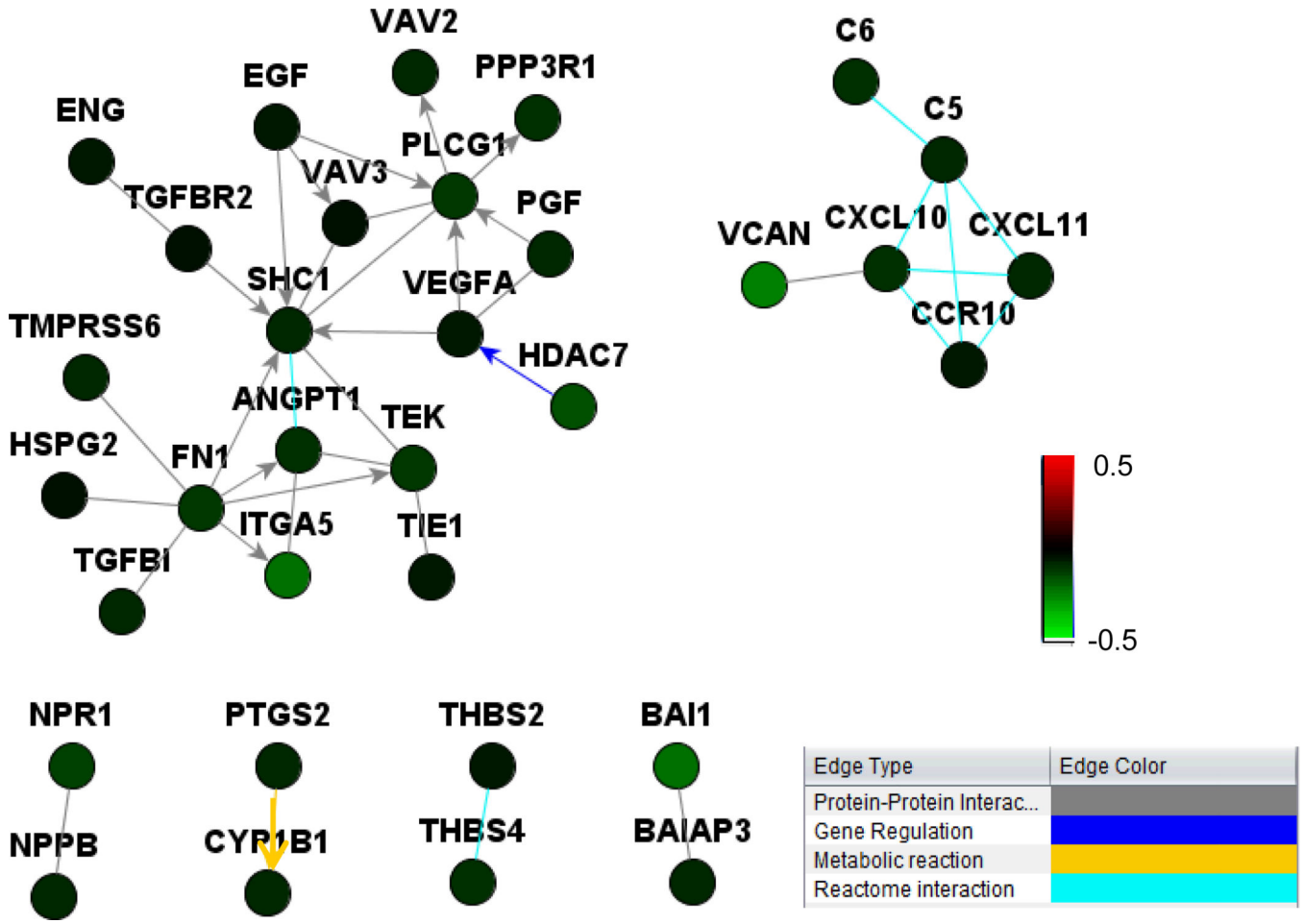

Figure 6. Network analysis of angiogenesis factors differentially regulated by 3G3 treatment in PDGFRa- positive cells (HEC-1A) and PDGFRa-negative cells (RL95-2)

Netwalker analysis showed that angiogenesis factors (e.g., VEGFA, HADC7, ITG, and VCAN) were down-regulated by 3G3 treatment in PDGFRa-positive cells, but not in PDGFRa-negative cells. Coloring is based on the log-ratio of expression levels for 3G3+PDGF-AA treatment over PDGF-AA treatment. Gene-expression differences were considered statistically significant if the *P* values were less than 0.001. A stringent significance threshold was used to limit the number of false-positive findings.